

J-PARC E16 Run0 proposal

S. Yokkaichi,^{1,*} K. Aoki,² S. Ashikaga,³ T. Chujo,⁴ H. En'yo,¹ S. Esumi,⁴ H. Hamagaki,⁵
R. Honda,⁶ M. Ichikawa,³ K. Kanno,⁷ Y. Komatsu,⁸ A. Kiyomichi,⁹ S. Miyata,⁷
Y. Morino,² H. Murakami,⁷ R. Muto,² W. Nakai,⁷ M. Naruki,³ H. Noumi,^{8,2}
K. Ozawa,^{2,7,4} T. Sakaguchi,¹⁰ H. Sako,¹¹ S. Sato,¹¹ F. Sakuma,¹ S. Sawada,²
M. Sekimoto,¹ K. Shigaki,¹² H. Sugimura,² T. N. Takahashi,⁸ and Y. S. Watanabe⁴

(J-PARC E16 Collaboration)

¹*RIKEN Nishina Center, RIKEN, 2-1 Hirosawa, Wako, Saitama 351-0198, Japan*

²*KEK, 1-1 Oho, Tsukuba, Ibaraki 305-0801, Japan*

³*Department of Physics, Kyoto University, Kitashirakawa Sakyo-ku, Kyoto 606-8502, Japan*

⁴*Center for Integrated Research in Fundamental Science and Engineering, University of Tsukuba, Tsukuba, Ibaraki 305-8577, Japan*

⁵*Institute for Innovative Science and Technology, Nagasaki Institute of Applied Science, 3-1, Shuku-machi, Nagasaki, 851-0121 Japan*

⁶*Department of Physics, Tohoku University, Sendai, 980-8578, Japan*

⁷*Department of physics, University of Tokyo, 7-3-1 Hongo, Tokyo 113-0033, Japan*

⁸*Research Center for Nuclear Physics (RCNP), Osaka*

University, 10-1 Mihogaoka, Ibaraki, Osaka, 567-0047, Japan

⁹*Japan Synchrotron Radiation Research Institute*

(JASRI), 1-1-1 Koto, Sayo, Hyogo 679-5198, Japan

¹⁰*Brookhaven National Laboratory, Upton, NY, 11973-5000, USA*

¹¹*Advanced Science Research Center, Japan Atomic Energy Agency, 2-4 Shirakata Shirane, Tokai-mura, Naka-gun, Ibaraki, 319-1195, Japan*

¹²*Graduate School of Science, Hiroshima University, 1-3-1 Kagamiyama, Higashi-Hiroshima 739-8526, Japan*

(Dated: June 26, 2017)

*spokesperson; yokkaich@riken.jp

Contents

Executive summary	2
1. Physics Motivation	3
2. Experiment	4
3. RUN 0: commissioning	8
3.1. Overview	8
3.2. Beam line commissioning	9
3.3. Detector commissioning	11
Appendix	15
A-1. Staging strategy	15
References	17

Executive summary

We have proposed the experiment E16 at J-PARC Hadron Experimental Facility to measure the vector meson decays in nuclei in order to investigate the spectral change of mesons and the chiral symmetry restoration in dense nuclear matter.

Since the stage-1 approval in 2007, we have developed detectors at RIKEN, U-Tokyo and KEK. GEM Tracker and Hadron Blind Čerenkov Detector using newly developed domestic GEMs are proved to work under the test using electron and pion beams. Lead-glass calorimeter is also tested. Readout circuit has been designed and a part of them are already prepared and tested.

Based on the recommendation by PAC-23, we would like to request the stage-2 approval of RUN 0 (beamline and detector commissioning run, 40 shifts, where '1 shift' means 8 hours.), with this revised proposal. We are preparing the experiment with the eight-module spectrometer, before the expected first beam of the high-momentum beam line in May 2019.

The detail of commissioning is described in section 3, following the sections of physics motivation and experimental overview. The staging strategy of this experiment after RUN 0 is described in Appendix.

1. PHYSICS MOTIVATION

We proposed an experiment E16 at J-PARC Hadron Experimental Facility to measure the vector meson decays in nuclei with the e^+e^- decay channel[1], in order to measure the spectral change of vector mesons in dense nuclear matter. The proposal of the experiment was submitted to the first J-PARC PAC and granted a stage-1 approval in March 2007. After that, we have developed detectors at RIKEN, University of Tokyo and KEK, with the support of Grant-in-Aid.

The aim of the experiment is to perform systematic studies of the spectral change of vector mesons, particularly the ϕ meson, in nuclei. The spectral change (or “mass modification”) of vector mesons in hot and/or dense matter is predicted by many theoretical approaches as nuclear many-body calculations, hadronic transport models, and so on [2, 3]. In general, spectral changes of the elementary excitation reflect the nature of vacuum on which the excitation is produced. Many measurements are performed on such phenomena in the field of condensed matter physics. In the present case, the excitation corresponds vector mesons (hadrons) and the vacuum corresponds a hot/dense QCD vacuum. From this point of view, there are calculations of spectral change of hadrons on the basis of the restoration of chiral symmetry in hot/dense QCD matter.

Many experimental studies have been conducted, even in dilepton invariant mass measurements, and the spectral changes in hot/dense matter have been observed. However, the origin of the changes has not yet been confirmed; in other words, there is no consensus on the interpretations of the phenomena. For example, in heavy-ion experiments, CERES [4], NA60 [5], STAR[6], and PHENIX [7, 8] have reported the low-mass enhancement in dilepton mass spectra. The former three stated that the spectra can be explained by the broadening of the ρ meson width, and recently, PHENIX data is also explained by the model[8]. Recently STAR reported a ϕ meson analysis that the width and mass are consistent with the natural ones [9]. In the lower energies, HADES experiment also reported the enhancement at low-mass region of the e^+e^- spectra, even in p+A reactions[10]. In the photon induced reaction, CLAS-g7 [11] experiment reported the width broadening of the ρ meson in the e^+e^- decay channel and explained it by the collisional broadening. And KEK-PS E325 [12–16], which was conducted by the collaboration including a part of the authors, measured e^+e^- invariant mass spectra in 12-GeV p+A reactions, and reported the enhancement on the low mass sides of ω and ϕ mesons, which are consistent with the mass decreasing of vector mesons predicted using QCD sum rule [17]. Only E325 can observe the mass-shape modification of a narrow resonance, ϕ , because they have the best mass resolution among above experiments, the better statistics than those of the photon-induced experiment, and the better signal-to-noise ratio than that of the heavy-ion experiments.

A goal of the present experiment is to measure the ϕ meson decays in the e^+e^- channel with the statistics that are two orders of magnitude larger than those of the experiment E325; namely, accumulate an order of 1×10^5 events for each nuclear target, H, C, Cu, and Pb. At the same time, the e^+e^- decays of the ρ , ω , and J/ψ mesons can be measured. However, the measurement of ϕ mesons is most notable because it is free from the ambiguity in the shape analysis as the ρ meson case; the complicated and broad mass shape even in vacuum, overlapping with the ω meson, and so on. With this amount of statistics, we can deduce the dependence of the shape modification on the matter size, and even on the meson momentum; the latter, which is the dispersion relation of vector mesons in matter, have never

been measured.

Such systematic studies enable us not only to confirm the E325 results but also to provide new systematic information of spectral change of vector mesons in nuclei, and to contribute to elucidate the nature of QCD vacuum.

2. EXPERIMENT

For the experiment, we will use a 30-GeV proton beam with an intensity of 1×10^{10} protons per pulse, at the high-momentum beam line, which is to be constructed at J-PARC Hadron Experimental Facility (Hadron hall). To increase the statistics by a factor of 100 compared to E325, the beam intensity is increased by a factor of 10, the acceptance of the spectrometer is enlarged to achieve a factor of 5, and the production cross section of the ϕ meson increase by a factor of 2, within the acceptance, by changing beam energy from 12 to 30 GeV. The target thickness must stay the same as E325, typically 0.1% interaction length and 0.5% radiation length, for each targets, typically C and Cu, to suppress the electron background caused by γ -conversion in the target. To cope with the expected interaction rate that is increased by a factor of 10, to 10-20 MHz, new spectrometer based on the new technology should be built. Also the readout circuits and DAQ system are prepared to take 1-2 kHz of trigger request within 80% live time, coping with the background from the 10-20 MHz interaction rate.

The schematic view of a proposed spectrometer is shown in Figure 1. Nuclear targets are located at the center of the spectrometer magnet. The primary proton beam is delivered on the target. GEM Tracker (GTR)[18, 19] which has three tracking planes is located around the target, between 200 mm and 600 mm in radius from the center of the magnet where the target is located. Outside the tracker, Hadron Blind Detector (HBD)[20–22] and lead-glass EM calorimeter (LG) are located successively to identify the electrons.

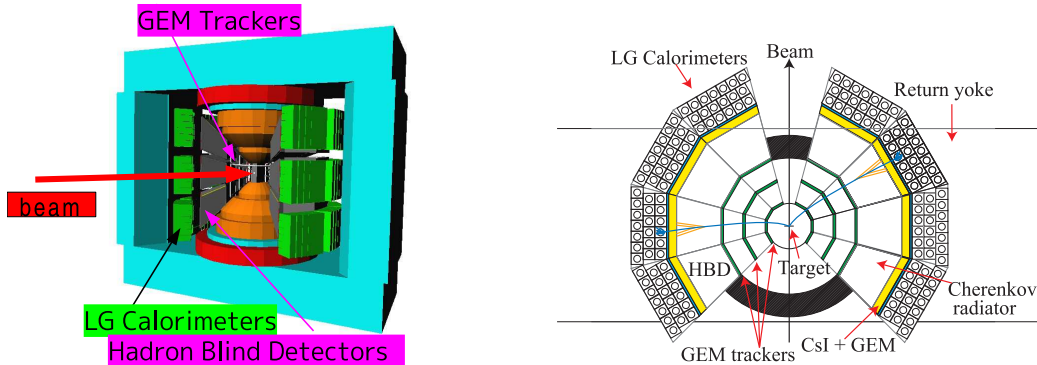


FIG. 1: Schematic view of the proposed spectrometer, the 3D view and the plan view.

GEM Tracker is required to cope with the high rate that is expected to reach 5 kHz/mm^2 at the most forward region of the proposed spectrometer. It should be noted that the COMPASS experiment reported that their GEM Tracker works under 25 kHz/mm^2 with a position resolution of $70 \mu\text{m}$ [23].

The goal of the mass resolution is $5 \text{ MeV}/c^2$, improved by a factor of two from that of E325, $11 \text{ MeV}/c^2$. With the resolution, possible double peak structure due to the modified ϕ mesons in nuclei could be observed by selecting very slowly-moving ϕ mesons, e.g. with a

momentum of less than 0.5 GeV/c. To achieve the mass resolution, a position resolution of 100 μm is required for the Tracker.

HBD is required to trigger the electron and positron tracks from vector meson decays with a larger acceptance and a finer trigger segment than that expected by the usual Čerenkov counter using PMT. The size of a trigger segment of HBD is about 100 mm \times 100 mm. To define an electron track candidate, a coincidence of a HBD segment and a LG block located just behind the segment is required with a corresponding hit on the most-outer GEM chamber of the Tracker (GTR3). Our goal of the pion rejection by the electron ID counters was approximately 10^{-3} in the trigger level and 10^{-4} in the offline analysis with a combination of HBD and LG. Based on the result of test experiments, we used the values of 0.2% (2% and 10% for HBD and LG) for online and 0.03% (0.6% and 5% for HBD and LG, with the electron efficiencies are 63% and 90%, respectively) for the offline analysis. These values are used for the background and yield estimation described in Appendix.

GEM Tracker, HBD and LG compose a detector module, as shown in Figure 1 schematically, which covers 30 degrees both horizontally and vertically around the target. A full spectrometer consists of 26 modules.

The drawing of the detectors in the spectrometer magnet is shown in Figs. 2, 3 and 4.

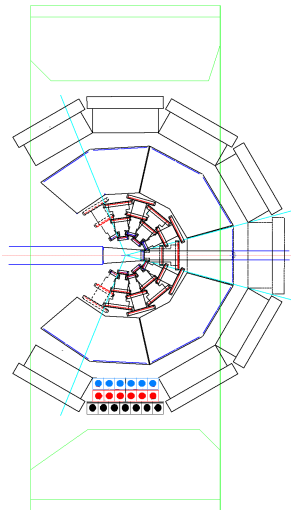


FIG. 2: Drawing of the spectrometer: plan view. Left is the upper stream of the beamline. The size of return yoke is approximately 2120 mm \times 5600 mm.

In actual design of the spectrometer, which are described precisely in the following sections, the three components are not connected mechanically, however, the GTRs are mechanically fixed to each other, in order to ensure the position alignment of each GEM Tracker. Each HBD and LG module cover approximately 30 \times 30 degrees, while each GTR module cover less than 30 degree because they are located in staggered form as described in Fig. 2 in order to minimize the dead region due to the frame of GEMs.

And also, three modules vertically stacked (upper, middle and lower) as shown in Figs. 3 and 4, due to the design of the mechanical support structure. Thus the vertical acceptance covered with the same GEM area is smaller than that of original design, in which the upper/lower modules are inclined by 30 degree against the vertical.

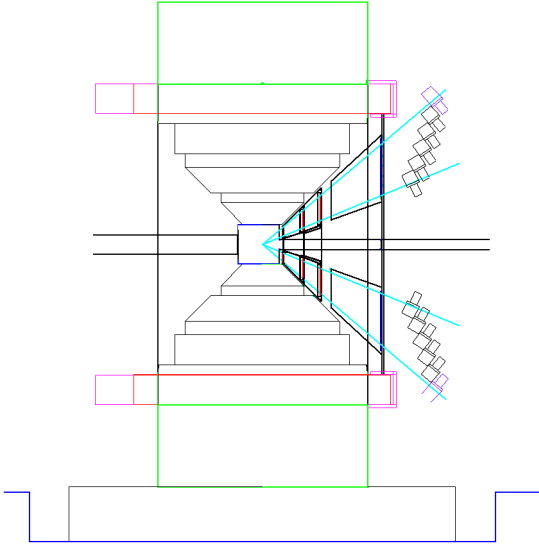


FIG. 3: Drawing of the spectrometer: elevation view along the beamline. Left is the upper stream. Green lines show the return yoke. Blue line shows the floor of Hadron Hall. The pit is located below the return yoke to fabricate the horizontal adjuster and supporting iron slab, which supports the large weight of the magnet (approximately 300 tons) by wider area. Red lines show the coils. Magenta square left of each coil, upper and lower, shows a pipe-space for the coil.

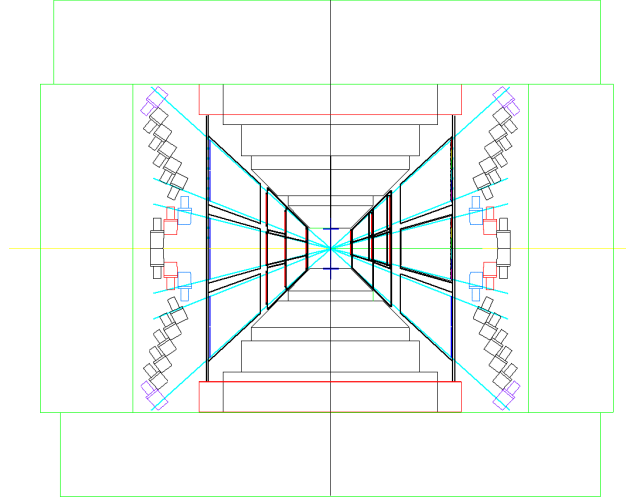


FIG. 4: Drawing of the spectrometer: elevation view from the upper stream of the beamline. Green lines show the return yoke and red lines show the coils.

By the Geant4 simulation, the mass resolution with the achieved GTR resolution is 5.4 MeV for the slowly-moving ϕ mesons which $\beta\gamma$ is less than 1.25, under the background-free environment. Under the high-background environment, and including possible alignment error of trackers, the resolution could be deteriorated to 7–8 MeV.

In addition above detectors, in order to improve the tracking performance under the expected high-background environment, we introduce a silicon strip detector as the inner tracker. Assumed specification is based on a SSD used by the J-PARC E10 experiment. Prof. Tanida from E10/E03 group agreed to provide their SSDs for the early stage of E16. By borrowing from him, we have an experience of operation of the SSDs, in our test experiment of GTR. Also, High- p collaboration agreement has been reached to develop SSDs together since not only E16, but also J-PARC E50 and J-PARC HI(heavy ion) group need SSDs. In the later stage of E16, we could use the newly prepared SSDs to cover the full acceptance.

For the spectrometer magnet, we will use so called 'FM magnet' used by KEK-PS E325, which was originally the FM-Cyclotron at INS, U-Tokyo [24].

We have prepared a coil which replace the broken one, a pair of pole pieces in order to increase the magnetic field, and expanding return yokes in order to increase the acceptance, with Grant-in-Aid[25] and they were delivered to the Hadron Hall in 2012. Re-construction of the magnet using the new parts was performed in 2015, as shown in the right side of Fig.5. The magnet is located at the proper location on the high-momentum beam line, where the

beam is delivered.

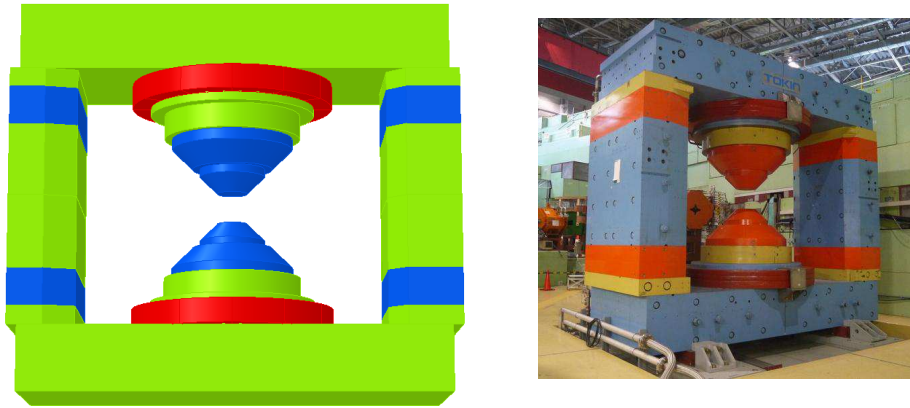


FIG. 5: Left: Design of Spectrometer magnet. The red parts are the coils and the blue parts are the additional pole pieces and yokes (see text). Right: A photograph of FM magnet after the reconstruction.

The drawing of the modified magnet is shown in Fig. 6.

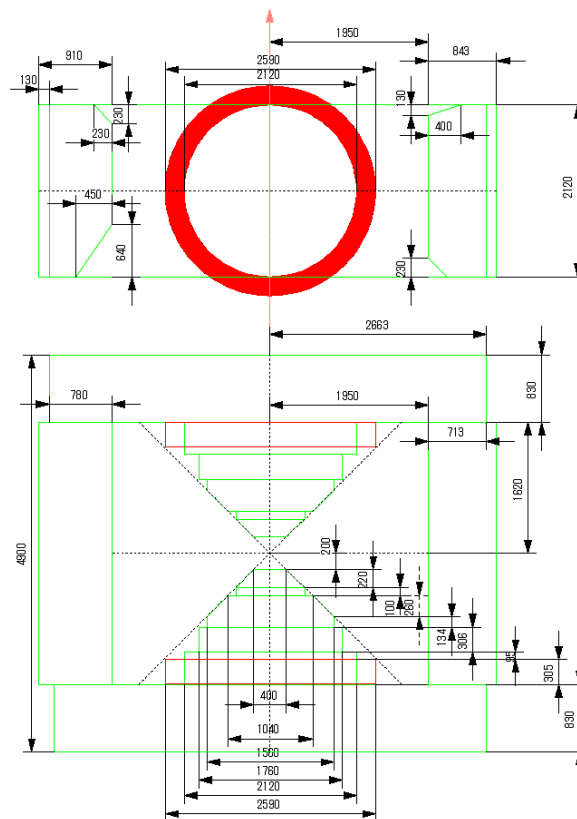


FIG. 6: The drawing of the modified FM magnet.

The maximum field strength is 1.7 T at the center of the magnet. The operation current is 2500 A (500V) with 168 turns of coil, thus 420000 A·turn is used. Three power supplies at J-PARC will be used in serial connection.

3. RUN 0: COMMISSIONING

3.1. Overview

The high-momentum (High-p) beam line under construction at J-PARC Hadron Experimental Facility is designed to provide a primary proton beam with the intensity of 1×10^{10} protons per spill (2-sec duration and 5.52-sec cycle).

RUN 0 is to be mainly dedicated for the commissioning of the beam line and the detectors. We request 40 shifts (where, 1 shift means 8 hours), 10 shifts for the beam line and 30 shifts for the detectors. We will use this opportunity to investigate various issues which should be cleared for detailed planning of the coming physics runs, particularly, the measurement of background environment. Also, the yield of vector mesons, namely, ρ , ω , and ϕ will also be measured. We would start with the 8-module configuration, as shown in Figs. 13 and 14, out of 26 modules of the full installation. At least we can start with the limited configuration shown in Fig. 12.

To deliver a first beam to the High-p beam line, beam tuning by the hadron beam line group will be performed. Following that, we would perform the study of beam line to measure and reduce the beam halo in 10 shifts of beam time. After that, we would perform the 30 shifts of detector commissioning. We expect these three periods are performed continuingly in a couple of months, with some short intervals, to perform the configuration change of detectors and so on.

We should consider two types of 'background' separately. One is the background appear in the e^+e^- invariant mass spectra, which lies underneath a meson resonance peak. Almost all of them are what we call 'combinatorial background', which originates from the combination of the uncorrelated pair of e^+ and e^- tracks including misidentified pion tracks. The main origins of the e^+ and e^- are π^0 Dalitz decay and the γ conversion in the materials of detectors and targets. The largest origin of γ is the π^0 decays.

The other is the accidental background hits in the detectors, particularly in the trackers. This could originate from the beam halo, room background from the beam dump etc., charged particles from the untriggered interactions on targets, and so on. The second type background depends on the condition of the constructed experimental area and evaluation is more difficult rather than the first one. We have evaluated the number of accidental hits using the data measured in the KEK-PS E325 experiment by scaling with the beam intensity, and have designed the detectors to cope with that. However, measurement of the real value in the RUN 0 is important and actually required by the J-PARC FIFC.

Brief description of effects of the accidental hits in our measurements is following, as illustrated in Fig. 7. The accidental hits increases the detector occupancy, especially of the SSD and of the GTR1 (first layer of the GEM Trackers), which are the two most inner layers of the tracking system. These hits are nothing to do with the tracks come from the interactions at the target which is of interest. However, the higher occupancy cause the higher probability of finding an accidental hit near a true hit of a true track in the triggered event. This will degrade the accuracy of the tracking and result in degraded momentum resolution.

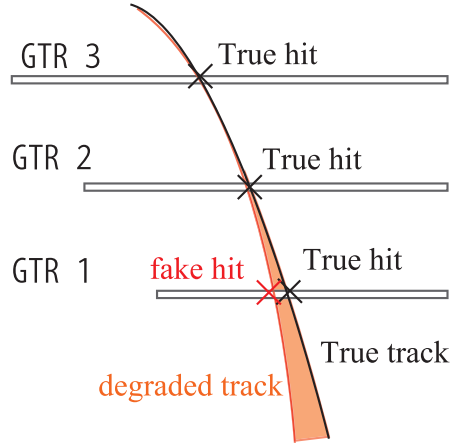


FIG. 7: Effect of high occupancy due to the accidental background hit. An accidental hit near the true hit (a track from the triggered event) results in a degraded track reconstruction.

3.2. Beam line commissioning

3.2.1. Purpose of beam line commissioning

One of the main purpose of RUN 0 data-taking is to measure a beam condition. We have two kinds of backgrounds in our measurements. As described in subsection 3.1, one is the background which will appear underneath a resonance peak. This background mainly consists of a combinatorial background. The other is the accidental hits which cause a miss-reconstruction of the interested tracks and degrade a detector performance. One of the origins of the accidental hits is a beam halo. The beam halo condition is difficult to estimate beforehand. Our current estimation of the beam halo is based on the KEK-PS E325 experience. However, the beam line itself is different. Thus, we need to measure the beam condition first.

To achieve the best experimental condition, we perform a beam commissioning in two steps.

- Beam Tuning
- Evaluation and minimization of beam backgrounds

The first part will be mainly performed by the hadron beam group collaborating with the E16 experimental group. The second part will be performed by the E16 group to achieve the best condition for our detectors.

3.2.2. Beam Tuning

Safe transports of the beam to experimental targets and a beam dump will be confirmed. Four monitors will be placed at the beam line to measure a beam profile. Using information of these monitors, beam transport will be checked carefully. The electrical current the beam line magnets will be adjusted slightly to meet a real situation, while initial values of the electrical current is determined by design calculations.

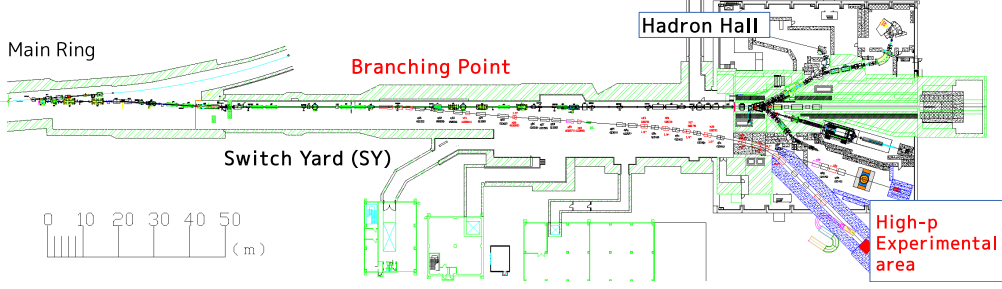


FIG. 8: High-p beam line, swithing yard, Hadron hall, and High-p experimental area.

In addition to the monitors, a fluorescent plate will be placed just before the target to check actual beam positions at the target. Also, we prepare the scintillator telescope consists of three scintillators in series aiming at the target to confirm the correct beam position using information of an interaction rate.

The beam tunings will be started with one-tenth of the nominal beam intensity, namely 1×10^{10} /spill, in case of unexpected errors of a beam tuning. After the confirmation of the beam conditions stated above, we will increase the beam intensity in steps.

The intensity of the high-p beam can be adjusted by a vertical position of the primary proton beam at a branching point from the main primary beam line, where a Lambertson-type septum magnet is placed. The branching point is located in the switching yard, about 100 m upstream of the T1 target of the main line as shown in Fig. 8. The Lambertson magnet, as shown in Fig. 9, has a large field-free area in a magnet pole and the great part of the primary beam enters to the field-free area and pass through straight. Tiny fraction of the primary beam enters to the pole gap and is bended to the high-p beam line. The beam intensity of the high-p beam line is determined by the fraction of the beam in the pole gap. The fraction can be adjusted by a vertical position of the primary beam.

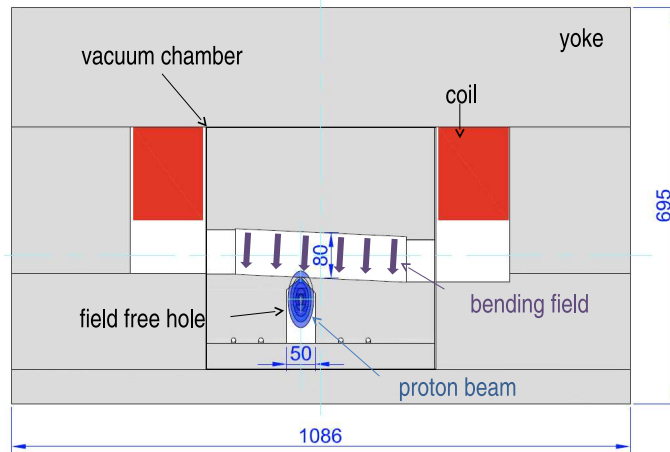


FIG. 9: A schematic view of the Lambertson septum magnet located at the branching point of the high-p beam line.

The beam intensity is measured by using an ion chamber. Stability of the beam intensity, beam conditions of the primary beam is carefully monitored.

This 'beam tuning' part is a part of machine developments and not included in our requested beam time.

3.2.3. Evaluation and minimization of beam backgrounds

The amount of the beam halo should be evaluated and minimized to perform our measurements effectively. To measure the beam halo, we prepare three scintillators in series and place them in parallel to the beam line near the target position. Three fold coincidence of the scintillators and the timing information will be used.

Minimization of the beam halo will be done by tunings of beam condition and collimator settings. The beam condition strongly depends on beam conditions of the primary beam, such as a beam orbit and emittance. The beam condition of the primary beam will be checked using the current monitors after installing the Lambertson magnet. The Lambertson magnet will be installed in 2018 and it is one year before the start of the high-p beam line commissioning. Based on measured information of the primary beam, several kinds of magnet current settings will be prepared to minimize the beam halo at the experimental area. To minimize the beam halo at the experimental area, it is important not to generate the beam halo at the upper stream. Thus, we should find out a magnet current setting to achieve a minimum loss at the first part of the high-p beam line. Small changes can cause a large difference in a beam loss. Thus, we need a enough time to have a trial and error. Collimators of the beam line are located in the switch yard and will be adjusted to minimize the beam halo also.

In addition to the beam halo, neutrons can come from a beam dump. There is a possibility to make hits on the detectors by neutrons. The neutron background from beam dump was estimated using MARS simulation. The estimated amount of the neutron is small enough compared to the beam halo background. The estimate should be confirmed with the real beam and we will measure them separately. For the neutron measurement, we put two thick scintillators at the downstream of detectors. If neutron background is not small enough, radiation shields will be added to suppress the neutron background to the sufficient level. Thus, it does not cause a serious problem.

3.3. Detector commissioning

In Run-0, we expect the 8-module configuration, as described in section 3.1.

We request 30 shifts of beam time for detector commissioning and yield measurements, which includes:

- Detector setup : 4 shifts
- Combined HBD and LG performance test : 6 shifts
- Zero field run for detector alignment : 4 shifts
- Tracking performance evaluation with various intensity : 7 shifts
- Data taking for measurement of meson yield: 9 shifts.

Detailed explanation of issues which need to be cleared follows.

3.3.1. Combined HBD and LG performance

The electron identification and pion rejection performance have to be evaluated using real data. Pion rejection of HBD and LG have been evaluated separately at test experiments, and proved to satisfy the required rejection factor. If there is some correlation of the responses between HBD and LG, rejection factor is less than the simple multiple of the independent two results. We think that the correlation between HBD (Gas Cherenkov) and LG (Leadglass electro-magnetic calorimeter) is not strong but has to be proved in a test experiment. We will prepare a special detector setup for this evaluation. A separate HBD and a LG are prepared so it can be done simultaneously with the main spectrometer. Figure 10 shows a schematic of the HBD-LG special setup. We will prepare two set of scintillators to define the test beam and between them two gas Cherenkov counters are placed in series to identify electrons and pions. Behind the beam defining setup, HBD and LG test modules are placed. Using 1×10^8 proton/spill or less, taking account of possible background in the forward area of targets, enough statistics can be collected within 6 shifts.

HBD has a fragile photo-cathode and it is difficult to test it outside of J-PARC, especially for a pion rejection factor as there is no hadron beam in japan for a suitable momentum range.

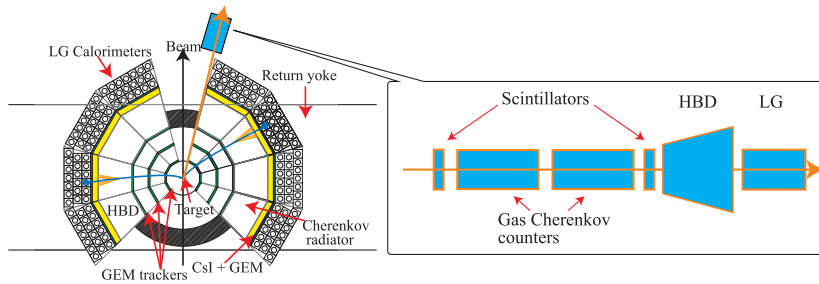


FIG. 10: Special setup for HBD-LG integrated performance test.

3.3.2. Integrated tracking performance (evaluation using physics signal)

The accuracy of magnetic field mapping and the detector alignment have to be confirmed using real data. The magnetic field has been calculated using a commercial software (Opera3D). The field will be measured with a Hall probe in advance. Using photogrammetry technique, the positions of outer layer detector components are precisely measured with an accuracy of $100 \mu\text{m}$. During the commissioning run, zero-field data will be taken for detector alignment. With the magnetic field on, the invariant mass of $K_s(497.6 \text{ MeV}/c^2)$ and $\Lambda(1115.7 \text{ MeV}/c^2)$ are reconstructed and peak position of these will be used to know the accuracy of the field mapping and detector alignment.

It is still challenging to find tracks under a high counting rate environment, even when we have SSDs. To evaluate the final yield precisely, tracking efficiency under the real condition should be known. Data will be taken under several different beam intensity to evaluate the background effect on tracking.

3.3.3. Zero field run

The displacement of the detectors are measured using straight track hit information obtained under zero-field. For this purpose, we will install four wire targets made of tungsten with diameters of 100 μm . Due to the thin wire targets, the vertex position of a straight track, which is unmeasurable directly, is restricted by the wire diameter. Therefore, based on straight track hits together with the vertex information, displacement of the positions of chambers can be determined. The setup is displayed in Fig. 11. Since the beam spot is about 10 mm, zero-field runs with two different beam positions will be performed: A run with the beam hitting on w1 and w2, and the other with the beam hitting on w3 and w4. For the alignment of a module, 1 M tracks are required. It takes 28 hours to collect enough statistics for 8-module configuration, with the beam intensity of 1×10^{10} protons per spill.

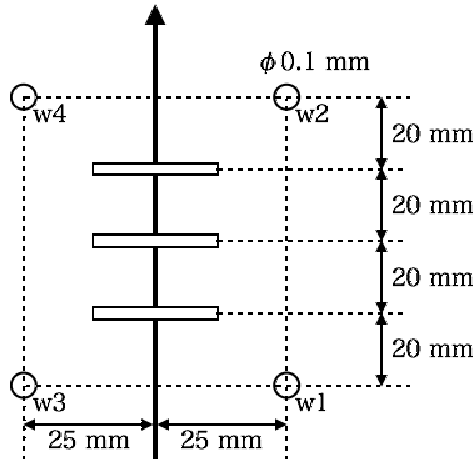


FIG. 11: Positions of the wire targets and the experimental targets. The thick arrow indicates the beam direction. The four circles represent wire targets with a diameter of 100 μm . The three boxes which the arrow penetrates are the experimental targets.

To estimate the required beam time for the zero-field run, GEANT4 simulation was performed. The major source of the straight tracks are the charged pions produced at the wire targets. Thus the cross section and the luminosity are necessary for the estimate and they are obtained as follows. The total cross section of charged pions is estimated based on the measured cross section of charged pion produced on Al target by 12.9 GeV/ c^2 proton beam which is 650 mb. [26] Assuming it scales as $A^{2/3}$ and $p^{0.7}$ where A denotes the mass number of the target and p represent the beam momentum, the cross section of charged pions ($\pi^+ + \pi^-$) is estimated to be 8.8 b. ¹ The momentum distributions of charged pions are taken from the nuclear cascade code JAM. [27]

The luminosity of the beam hitting on a wire target, L , is calculated as

$$L = \frac{\dot{N}_a}{\sqrt{2\pi}\sigma} \pi r^2 n_b = \dot{N}_a n_b \times 0.002[\text{mm}], \quad (1)$$

where \dot{N}_a is the number of the beam particles per unit time (10^{10} /spill), r is the radius of the wire target (0.05 mm), n_b is the number density of the wire target, and σ is the horizontal

¹ The value is 77% of the result of JAM.

width of the beam. The horizontal distribution of the beam is assumed to be a Gaussian with a width of $\sigma = 1.5$ mm. In this calculation, the beam density is approximated by its peak value since the width is much larger than the wire radius. Therefore, the luminosity is equivalent to the case of a large flat-plate target which is 0.002 mm thick. Thus the interaction rate is approximately 200 kHz taking account of the beam intensity of 1×10^{10} protons /spill(2-sec) and the two wires are simultaneously in the beam.

3.3.4. Trigger condition

The main sources of fake triggers are γ conversion and π^0 Dalitz decays at the upstream of the target chamber and chance coincidence of e^+e^- pairs from two independent π^0 Dalitz decays and/or γ conversions. This really depends on the beam conditions, spectrometer configurations and beam intensity. Therefore, our evaluations should be confirmed by measurements.

3.3.5. Yield and distribution

For the evaluation of the final yield, production yield and rapidity/ p_T distribution of $\rho/\omega/\phi$ at nuclear targets are basic information and it will be measured. Currently, we use an evaluation based on the measurement by KEK-PS E325[15] and calculation with JAM.

In the 9 shifts (72 hours) of data taking with 8 detector modules, we expect to obtain approximately 4400 ω and 840 ϕ mesons for the Cu target, and the almost same order of that for C target. In this estimate, production cross sections of vector mesons are based on the E325 result (12 GeV p+A reaction) and extrapolated to 30 GeV case using JAM. The result of 30 GeV p+Cu reaction in JAM is scaled by a factor : [measured cross section by E325]/[12 GeV JAM cross section], which is approximately 41% and 71% for ω and ϕ , respectively. This evaluation should be checked by the data.

Appendix

A-1. Staging strategy

Here, we describe our strategy towards the final goal. We adopt a staged approach in the construction of the spectrometer. According to the latest construction plan of the beam line, the high- p experimental area accepts the primary proton beam for the first time in May 2019. The currently secured budget allows us to build and install 6 modules of SSDs, 6 of GTRs, 2 of HBDs, and 2 of LGs by Jan. 2019. It is well before the anticipated construction schedule of the beam line and the spectrometer itself becomes ready for the beam time earlier if the construction schedule of the beam line is moved forward. The configuration is schematically shown in Fig. 12. The secured budget includes Grant-in-Aid Shin-gakujutsu (FY2009-2013), Kiban-A (FY2014-2016), Wakate-B (FY2014-2016), and Wakate-A (FY2015-2017). We consider application of other Grant-in-Aid and if we get support in a timely fashion, we can extend the acceptance. With an additional budget of 0.9 Oku yen, we are able to prepare 8 of SSDs, 8 of GTRs, 8 of HBDs, and 8 of LGs and the configuration is illustrated in Fig. 13 and Fig. 14.

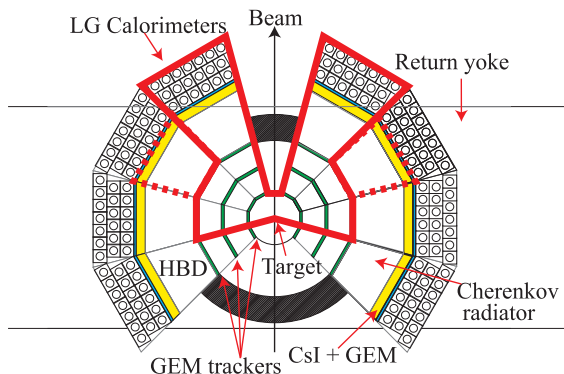


FIG. 12: Detector configuration in RUN 0 based on the secured budget. 6 of SSDs (not visible), 6 of GTRs, 2 of HBDs, 2 of LGs.

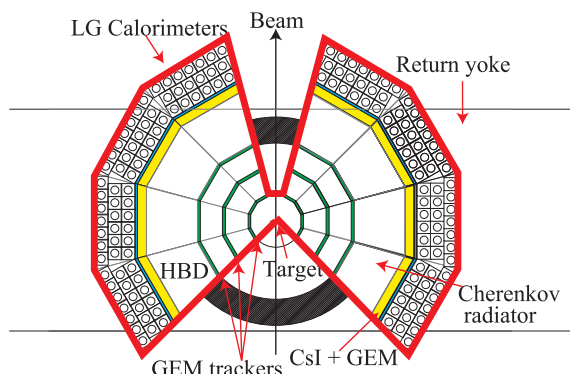


FIG. 13: Detector configuration in RUN 0 with an additional budget. 8 of SSDs, GTRs, HBDs, and LGs.

The re-construction of FM magnet with newly added parts completed in 2015. We will install the detector components available at the time of installation and do necessary adjustments to accept the first beam planned in May 2019.

We request 40 shifts of beam time and we call it RUN 0. We would like to use this opportunity for the commissioning of the beam line and the detectors, and measurement of the yields of ρ , ω , and ϕ . Detailed plan of RUN 0 is described in section 3.

We plan to request 160 shifts scheduled during the next SX (slow extraction) run period of J-PARC MR, in late 2019 or 2020, and we call it RUN 1. We will take physics data and investigate spectral change of vector mesons ρ , ω and ϕ . We will accept the beam with at least 6 of SSDs, 6 of GTRs, 2 of HBDs, and 2 of LGs. Depending on the budget, we maybe able to extend the acceptance and prepare 8 of SSDs, 8 of GTRs, 8 of HBDs, and 8 of LGs.

In this stage, we can confirm the results by the precedent experiment, KEK-PS E325, and further, the first data of momentum dependence of the spectral change, with the 6 times

higher statistics than that of E325 collected, as shown in this section. In addition, we also measure the yield and kinematical distribution of vector mesons, and background conditions in the limited detectors in this stage. Based on the information, we could bluish up the detailed plan of the next stage.

With additional budget of about 5 Oku yen, we will be able to prepare the full acceptance, which consists of 26 modules. (Cost for new module is 0.26 Oku yen/module including readout electronics.) The configuration is illustrated in Fig. 15. We would like to run 320 shifts (RUN 2) with the configuration, and take physics data. We will be able to do systematic study of the in-medium spectral change of vector mesons.

The expected yield of vector mesons expected for the different configuration and different lengths of the data taking is listed in Table I. For the estimation, we assume the usage of a 400 μm -thick Carbon target and two 80 μm -thick Copper targets simultaneously, located in-line on the beamline. Thus the total interaction length is 0.2 % and the interaction rate is 10 MHz at the target with the beam of 1×10^{10} protons per 2-sec pulse. Other numbers used for the yield estimation is summarized in Table II.

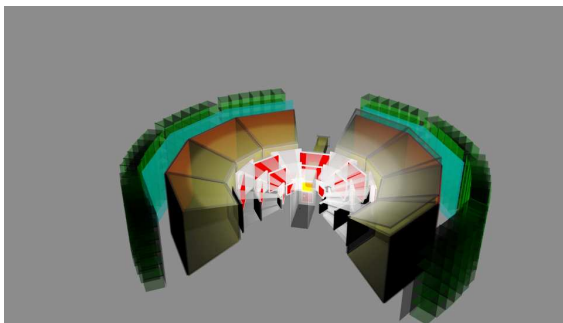


FIG. 14: Detector configuration with 8 modules.

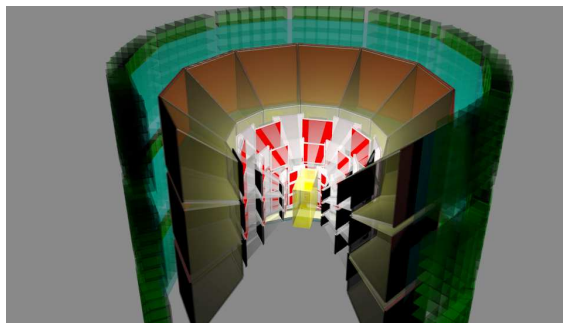


FIG. 15: Detector configuration with 26 modules. (RUN 2)

RUN	beam time	configuration	target	ϕ	ω
RUN 0	9 shifts	6 + 6 + 2 + 2	Cu	460	2400
RUN 0'	9 shifts	8 + 8 + 8 + 8	Cu	840	4400
RUN 1	160 shifts	6 + 6 + 2 + 2	Cu	8200	42000
RUN 1'	160 shifts	8 + 8 + 8 + 8	Cu	15000 (1700)	
RUN 1''	160 shifts	8 + 8 + 8 + 8	C	12000 (1500)	
RUN 2	320 shifts	26 + 26 + 26 + 26	Cu	69000 (12000)	
		KEK-PS E325	Cu	2400 (460)	3200

TABLE I: Numbers of ϕ 's and ω 's expected for different configurations and lengths of the beam time, compared to the numbers obtained by the KEK-PS E325 experiments. Numbers in parentheses are for mesons with $\beta\gamma < 1.25$. Four numbers interleaved with “+” in the configuration column describes the numbers of the modules for the four spectrometer components : SSD, GTR, HBD, and LG, respectively.

Responsible person for each detector subsystem in the collaboration are summarized in table III.

production cross section of ϕ meson	4.8 mb 1.2 mb	30 GeV p+Cu, scaled from the data by E325[15] 30 GeV p+C
branching ratio $\phi \rightarrow e^+e^-$	2.95×10^{-4}	PDG 2016
Cu target thickness [atom/cm ²]	1.35×10^{21}	80 $\mu\text{m} \times 2$
C target thickness [atom/cm ²]	4.55×10^{21}	400 μm
protons/spill	1×10^{10}	2 sec duration
spill/hour	652	5.52 sec cycle
beam available time	70%	beam down, DAQ down, calib. run, etc.
DAQ live time	76%	SRS 1 kHz request
electron ID efficiency (HBD)	63%	for single track
electron ID efficiency (LG)	90%	for single track
GTR trigger efficiency	88%	for a pair
Trigger logic efficiency	74%	applied only for the full detectors to reduce the trigger request to 1 kHz
detector acceptance	1.45%	including SSD, 8 module configuration
pair reconstruction efficiency	43%	under the expected background with 1×10^{10} beam

TABLE II: Numbers used for the yield estimation in this section.

GEM Tracker	S. Yokkaichi (RIKEN Nishina Center)
Hadron Blind Detector	K. Aoki (KEK IPNS)
Lead Glass Calorimeter	M. Naruki (Kyoto-U)
Silicon Strip Detector	H. Noumi (RCNP, Osaka-U)
DAQ/electronics	K. Ozawa (KEK IPNS)
Software	S. Yokkaichi (RIKEN Nishina Center)
High-p Beam line	K. Ozawa (KEK IPNS)
Site Management	K. Aoki (KEK IPNS)

TABLE III: Responsible person for each detector subsystem.

-
- [1] S. Yokkaichi *et al.*, J-PARC proposal No. 16
http://j-parc.jp/researcher/Hadron/en/pac_0606/pdf/p16-Yokkaichi_2.pdf,
Lect. Notes Phys. **781**, 161-193 (2009).
- [2] R. S. Hayano and T. Hatsuda, *Rev. Mod. Phys.* **82**, 2949 (2010).
- [3] S. Leupold, V. Metag and U. Mosel, *Int. J. Mod. Phys.* **E19**, 147 (2010).
- [4] G. Agakichiev *et al.* (CERES Collaboration), *Phys. Rev. Lett.* **75**, 1272 (1995).
G. Agakichiev *et al.* (CERES Collaboration), *Euro. Phys. J. C* **41**, 475 (2005).
D. Adamova *et al.*, (CERES Collaboration), *Phys. Lett.* **B 666**, 425 (2009).
- [5] R. Arnaldi *et al.*, *Phys. Rev. Lett.* **96**, 162302 (2006).
S. Damjanovic for the NA60 Collaboration, *Nucl. Phys. A* **783**, 327 (2007).
- [6] L. Adamczyk *et al.* (STAR Collaboration), *Phys. Rev. Lett.* **113**, 022301 (2014).
- [7] A. Adare *et al.* (PHENIX Collaboration), *Phys. Rev. C* **81**, 034911 (2010).
- [8] A. Adare *et al.* (PHENIX Collaboration), *Phys. Rev. C* **93**, 014904 (2016).
- [9] L. Adamczyk *et al.* (STAR Collaboration), arXiv:1503.04217
- [10] G. Agakishiev *et al.* (HADES Collaboration), *Phys. Lett. B* **715**, 304 (2012).
- [11] R. Nasseripour *et al.* (CLAS Collaboration), *Phys. Rev. Lett.* **99**, 262302 (2007).
M. H. Wood *et al.* (CLAS Collaboration), *Phys. Rev. C*, **78**, 015201 (2008).

- [12] K. Ozawa *et al.*(KEK-PS E325 Collaboration), *Phys. Rev. Lett.* **86**, 5019 (2001).
- [13] M. Naruki *et al.*(KEK-PS E325 Collaboration), *Phys. Rev. Lett.* **96**, 092301 (2006).
- [14] R. Muto *et al.*(KEK-PS E325 Collaboration), *Phys. Rev. Lett.* **98**, 042501 (2007).
- [15] T. Tabaru *et al.*(KEK-PS E325 Collaboration), *Phys. Rev. C* **74**, 025201 (2006).
- [16] F. Sakuma *et al.*(KEK-PS E325 Collaboration), *Phys. Rev. Lett.* **98**, 152302 (2007).
- [17] T. Hatsuda and S. H. Lee, *Phys. Rev. C* **46**, R34 (1992), T. Hatsuda, S. H. Lee and H. Shiomi, *Phys. Rev. C* **52**, 3364 (1995).
- [18] F. Sauli, *Nucl. Instrum. Meth. A* **386**, 531 (1997).
- [19] Y. Komatsu *et al.*, *Nucl. Instrum. Meth. A* **732**, 241-244 (2013).
- [20] Y. Giomataris and G. Charpak, *Nucl. Instrum. Meth. A* **310**,589 (1991).
- [21] A. Kozlov *et al.*, *Nucl. Instrum. Meth. A* **523**, 345 (2004).
- [22] K. Kanno *et al.*, *Nucl. Instrum. Meth. A* **819**, 20-24 (2016).
- [23] B. Ketzer *et al.*, *Nucl. Instrum. Meth. A* **535**, 314 (2004).
- [24] I. Katayama and T. Shibata, *Butsuri* **49**, 200 (1994).
- [25] Grant-in-Aid for Scientific Research on Innovative Areas 2104: “Elucidation of New hadrons with a Variety of Flavors”,
http://www.hepl.phys.nagoya-u.ac.jp/public/new_hadron/index-e.html
- [26] M.G.Catanesi *et al.*(HARP Collaboration), *Euro. Phys. J. C* **54**, 37 (2008).
- [27] Y. Nara *et al.*, *Phys. Rev. C* **61**, 024901 (2000).